

---

# VeFA: Vector-Based Feature Space Adaptation for Robust Model Fine-Tuning

---

**Peng Wang**

University of Southern California  
pwang341@usc.edu

**Minghao Gu**

University of Southern California  
minghaog@usc.edu

**Qiang Huang \***

University of Southern California  
qiang.huang@usc.edu

## Abstract

Catastrophic forgetting is a well-documented challenge in model fine-tuning, particularly when the downstream domain has limited labeled data or differs substantially from the pre-training distribution. Existing parameter-efficient fine-tuning methods largely operate in the weight space by modifying or augmenting the pre-trained model’s parameters, which can lead to models that are overly specialized to the observed downstream data. Recent studies suggest that one mechanism underlying such forgetting is the introduction of intruder dimensions into the representation space during fine-tuning. To mitigate the risk of overwriting pre-trained knowledge and to enhance robustness, we propose Vector-based Feature Space Adaptation (VeFA), a new fine-tuning method that operates directly in the feature space, which naturally avoids generating intruder dimensions. VeFA performs element-wise adaptation on individual features, thereby ensuring that the effective fine-tuned weights always remain within the column space of the pre-trained weight matrix. This feature-space adaptation perspective is inspired by the idea of effect equivalence modeling (EEM) of downstream lurking variables that induce distribution shifts, which posits that the influence of unobserved factors can be represented as an equivalent aggregate effect on observed features. By compensating for the effects of downstream lurking variables via a lightweight feature-level transformation, VeFA preserves the pre-trained representations and improves model generalization under distribution shift. We evaluate VeFA against LoRA on image classification, NLU, and NLG benchmarks, considering both standard fine-tuning performance and robustness; across these tasks, VeFA achieves comparable fine-tuning performance while consistently exhibiting stronger robustness.

## 1 Introduction

Pre-trained models on large-scale datasets have demonstrated strong generalization and transferable representations across a wide range of downstream domains and tasks [1]. However, due to distributional differences between the pre-training and downstream data, it is often necessary to fine-tune the pre-trained model. For example, a vision–language model such as CLIP [2], pre-trained on web-scale image–text pairs, can be fine-tuned on Oxford-IIIT Pets for species recognition. Similarly, a language model such as GPT-2 [3], pre-trained on broad web text, can be fine-tuned on WebNLG [4] for data-to-text generation. This pretraining-to-fine-tuning paradigm enables efficient knowledge transfer and is especially beneficial when downstream labels are scarce.

Fine-tuning is typically achieved by adjusting the pre-trained model in the weight space to better align with the distribution and characteristics of the downstream data [5]. Traditional methods include full fine-tuning and linear probing [6]. Full fine-tuning updates all the parameters of the pre-trained model using the downstream task data. Linear probing updates only the final linear layer—the “head”—on top of the frozen pre-trained features. To balance adaptation capability and efficiency, parameter-efficient fine-tuning (PEFT) methods have received increasing attention in recent years [7–9]. Among PEFT methods, LoRA [9] is particularly influential: it injects low-rank update matrices into frozen weights and achieves strong downstream adaptation. These approaches go beyond linear probing while avoiding the computational and overfitting costs of full fine-tuning.

Since current fine-tuning methods primarily adapt the pre-trained model in the weight space, they allow the learned representations to exit the column space induced by the pre-trained weight matrix, thereby introducing intruder dimensions [10] that were not present in the original pre-trained subspace. This subspace escape increases expressivity and enables a tighter fit to the downstream data, but it also risks overwriting the general representations acquired during pre-training and can lead to overfitting, particularly in low-resource settings. This phenomenon is commonly referred to as catastrophic forgetting [11–14]. For example, fine-tuning a pre-trained model on a specific downstream domain often degrades its zero-shot performance on other domains [15], reflecting a loss of the broad generalization capability originally obtained during pre-training.

Weight-space fine-tuning methods typically assume that the input–output mapping learned during pre-training is insufficiently aligned with the downstream dataset. Consequently, they replace the pre-trained weights  $\mathbf{W}_0$  with adapted weights  $\mathbf{W}'$  to achieve effective adaptation. However, the discrepancy between the pre-training dataset and the downstream dataset is often unknown or unmeasurable. Fine-tuning model in the weight space using limited downstream data cannot avoid the large modification of partial model parameters and therefore risk the change of learned knowledge during pre-training stage. **The fundamental question becomes how to represent and integrate the unobservable downstream data discrepancy into the pre-trained model.**

Instead of modifying weights in the weight space, we propose to fine-tune in the feature space. The central insight is to constrain adaptation so that the fine-tuned model always remains within the column space of the pre-trained  $\mathbf{W}_0$ . This guarantees that downstream updates cannot drift away from the representational subspace established during large-scale pre-training, thereby better preserving the broad knowledge already encoded. Although such feature-space adaptation nominally reduces the expressive power compared to unconstrained weight-space updates, the over-parameterization of modern neural networks ensures that there is still ample capacity to fit downstream tasks [12], enabling fine-tuned models to achieve comparable performance while exhibiting consistently stronger robustness. This design is further motivated by the fact that pre-training typically involves data that are orders of magnitude larger and more diverse than any downstream task, endowing the model with strong generalization and even zero-shot capability. Fine-tuning should therefore respect and leverage the structure embedded in  $\mathbf{W}_0$ , rather than overwriting it, ensuring stability while still accommodating downstream-specific shifts.

The feasibility of feature-space adaptation is grounded in the idea of effect equivalence modeling (EEM) for lurking variables: given observed inputs and outputs, EEM compensates the influence of unobservable downstream factors by mapping their effect onto the observed features within the column space of the pre-trained weights. The unobservable factors that cause domain discrepancy can be more formally described as lurking variables in statistics [16, 17]. A lurking variable is defined as a variable that has an important effect but is not included among the predictor variables under consideration. It may be omitted from the analysis because its existence is unknown, its influence is assumed to be negligible, or relevant data are unavailable [18]. As illustrated in Fig. 1, lurking variables  $\mathbf{U}$  can alter the probability distributions of both the input  $\mathbf{X}$  and the response  $\mathbf{y}$  in the observed data, thereby affecting the observed association between them. This leads to a perceived inconsistency between the downstream data and the pre-trained data. By identifying the equivalent amount  $\Delta$  of lurking variable effects through input transformation, the pre-trained model can be more effectively applied to the downstream domain without modifying its parameters.

Lurking variables are ubiquitous across application domains. In computer vision, factors such as style, texture, or lighting conditions can act as lurking variables, systematically altering observed features while remaining unobserved and unlabeled during training [19]. In natural language processing, language type or domain (e.g. news versus reports) influences syntactic and lexical patterns, yet is

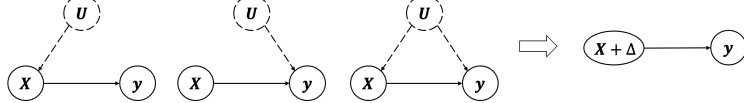


Figure 1: Three types of lurking variable impacts and their equivalent transformation

often ignored in modeling [20]. More generally, distributional discrepancies between pre-training datasets (e.g., ImageNet, Wikipedia) and downstream benchmarks (e.g., Oxford Pets, CoLA) can be viewed as arising from lurking variables that confound the input–output relationship. In manufacturing applications, unobservable process changes such as machine calibration have been modeled as lurking variables in 3D printing quality control [21, 22]. In causal inference, unmeasured confounding remains the classical example of lurking variables, extensively studied in synthetic control [23].

The remainder of the paper is organized as follows. In Section 2, we formally review the framework of EEM for lurking variables, which provides the theoretical foundation of our study. In Section 3, we present how EEM can be applied to design a new fine-tuning strategy that mitigates catastrophic forgetting. The effectiveness of the proposed approach is demonstrated through empirical evaluations in Section 4, followed by conclusions and future directions in Section 5.

## 2 Preliminaries

### 2.1 Intruder Dimension

[10] introduces a new concept, called *intruder dimension*, and discusses its impact on LoRA forgetting. Its detailed experimental analysis provides valuable evidence that LoRA introduces new intruder dimensions outside the span of the principal singular vectors of  $\mathbf{W}_0$ . These intruder directions lie beyond the main representational subspace of the pre-trained model and can therefore contribute to catastrophic forgetting.

Here, we give a formal definition of intruder dimension. Let  $\mathbf{W}_0 = \mathbf{U}_0 \Sigma_0 \mathbf{V}_0^\top$ ,  $\mathbf{W}_p = \mathbf{U}_p \Sigma_p \mathbf{V}_p^\top$ . Define  $\mathcal{S}_0 = \text{span}(\mathbf{U}_0[:, 1:r_0])$ ,  $\mathcal{S}_p = \text{span}(\mathbf{U}_p[:, 1:r_p])$ , where  $r_0, r_p$  are

$$r_0 = \inf \left\{ r \in \mathbb{Z} : \sum_{i=1}^r \sigma_{0,i}^2 \geq \alpha \|\mathbf{W}_0\|_F^2 \right\}, \quad r_p = \inf \left\{ r \in \mathbb{Z} : \sum_{i=1}^r \sigma_{p,i}^2 \geq \alpha \|\mathbf{W}_p\|_F^2 \right\},$$

i.e., the first  $r_0$  or  $r_p$  singular vectors capture at least an  $\alpha$  fraction of the total spectral power (sum of squared singular values). We need to define  $r_0$  and  $r_p$  because in practice, a pre-trained / fine-tuned weight matrix is not full rank in an effective sense: its tail singular values are very small (e.g.  $1 \times 10^{-5}$ ). Thus, we only need to focus on the directions that carry most of the energy, for example those whose squared singular values account for at least an  $\alpha$  fraction (e.g.,  $\alpha = 0.99$ ) of the total spectral power. A unit vector  $\mathbf{u} \in \mathcal{S}_p$  is an *intruder dimension* of  $\mathbf{W}_p$  w.r.t.  $\mathbf{W}_0$  if  $\|P_{\mathcal{S}_0} \mathbf{u}\|_2^2 < \varepsilon$ , where  $P_{\mathcal{S}_0}$  is the orthogonal projector onto  $\mathcal{S}_0$ . In this paper, we will establish a mathematical link between intruder dimensions and catastrophic forgetting, and propose a principled approach to mitigating the impact of such intruder dimensions.

### 2.2 Effect Equivalence Modeling of Lurking Variables

In modeling a system’s responses  $\mathbf{y} \in \mathbb{R}^k$ , it is useful to distinguish two categories of influencing variables: (i) observable variables  $\mathbf{X}$  that are measured and available for analysis, and (ii) lurking variables  $\mathbf{U}$  that are unobserved, ignored, or lack corresponding data yet may introduce variability [16, 18]. Standard assumptions typically treat  $\mathbf{X}$  as the sole explanatory factors and regard  $\mathbf{U}$  as fixed or negligible. Under these assumptions, the system is modeled as  $\mathbf{y} = f(\mathbf{X}) + \epsilon$ , where  $f : \mathbb{R}^d \rightarrow \mathbb{R}^k$  denotes the response map and  $\epsilon$  is a  $k$ -dimensional noise term ( $\mathbb{E}[\epsilon] = \mathbf{0}$  and  $\text{Cov}(\epsilon) = \Sigma$ ). However, when such assumptions are violated (more aligned with real-world scenarios such as the downstream data with unknown discrepancy with the pre-training data), the response should instead be modeled as

$$\mathbf{y} = g(\mathbf{X}, \mathbf{U}) + \epsilon \tag{1}$$

where lurking variables  $\mathbf{U}$  exert non-negligible influence. Lurking variables pose one central challenge in research: how to infer and account for their effects when direct observation is not accessible.

When the usual assumptions are met, Eq. 1 is degenerated into Eq. 2 and  $f(\cdot)$  has a simpler form.

$$\mathbf{y} = g(\mathbf{X}, \mathbf{U} = \mathbf{0}) + \epsilon = f(\mathbf{X}) + \epsilon \quad (2)$$

However, when lurking variables are present and exert significant effects, directly applying Eq. 2 can lead to biased predictions of the system. To address this issue, we propose EEM to model the effects of lurking variables.

**Definition 1 (EEM).** Let  $g : \mathbb{R}^d \times \mathbb{R}^m \rightarrow \mathbb{R}^k$  be a  $k$ -dimensional response function defined on observable variables  $\mathbf{X}$  and lurking variables  $\mathbf{U}$ . Assume  $g \in C^1(\mathbb{R}^d \times \mathbb{R}^m)$  and that for each  $i \in \{1, \dots, d\}$ , the partial derivative  $\frac{\partial g}{\partial x_i}(\mathbf{X}, \mathbf{0}) \in \mathbb{R}^k$  is non-zero. The total equivalent amount of lurking-variable effects  $\Delta$  in terms of  $\mathbf{X}$  can then be estimated from the data.

$$g(\mathbf{X}, \mathbf{U}) = g(\mathbf{X} + \Delta, \mathbf{U} = \mathbf{0}) = f(\mathbf{X} + \Delta) \quad (3)$$

The justification follows from the mean value theorem applied to a first-order Taylor expansion. There is no explicit solution for  $\Delta$ , but it can be estimated through statistical learning or neural networks using the observed variables  $\mathbf{X}$  as input.

Lurking variables explain the source of discrepancy between the pre-training dataset and the downstream dataset: unobserved or missing features prevent the pre-trained model from being directly applied to the downstream domain or task. EEM provides a solution to mitigate the influence of lurking variables and also offers a perspective for performing fine-tuning in the feature space without changing model parameters.

### 3 Methodology

#### 3.1 Problem Setup

We evaluate the robustness of fine-tuning methods using the established criteria from the literature: fine-tuning within a single downstream dataset/task should not reduce accuracy on other downstream datasets/tasks compared with zero-shot models [15].

Firstly, we present the general formulation for model fine-tuning. Let  $f_{\mathbf{W}_0} : \mathcal{X} \rightarrow \mathcal{Y}$  be a pre-trained model with parameters  $\mathbf{W}_0$ . Given a downstream training set  $\mathcal{D}_{\text{tr}}$ , fine-tuning solves

$$\mathbf{W}_p = \arg \min_{\mathbf{W} \in \mathcal{A}} \mathcal{L}(\mathbf{W}; \mathcal{D}_{\text{tr}}), \quad \mathcal{L}(\mathbf{W}; \mathcal{D}_{\text{tr}}) = \mathbb{E}_{(\mathbf{X}, \mathbf{y}) \sim \mathcal{D}_{\text{tr}}} [\ell(\mathbf{X}, \mathbf{y}; f_{\mathbf{W}})],$$

where  $\mathcal{A}$  encodes the adaptation family (e.g., full FT and LoRA) and  $\mathcal{L}(\mathbf{W}; \mathcal{D}_{\text{tr}})$  denotes the loss function of  $\mathbf{W}$  for fine-tuning dataset  $\mathcal{D}_{\text{tr}}$ .

In practice, the choice of loss function  $\mathcal{L}$  depends on the downstream task: cross-entropy is typically used for classification, mean squared error for regression, and token-level negative log-likelihood for natural language generation tasks.

For full FT,  $\mathbf{W}$  is initialized at the pre-trained parameters  $\mathbf{W}_0 = \{\mathbf{W}_0^{(l)}\}_{l=1, \dots, L}$  (where  $L$  denotes the number of learnable layers in the pre-trained model), and update all components end to end. For LoRA, each layer weight  $\mathbf{W}_0^{(\ell)} \in \mathbb{R}^{p \times q}$  is frozen and augmented with a low-rank update  $\mathbf{B}^{(\ell)} \mathbf{A}^{(\ell)}$ , where  $\mathbf{A}^{(\ell)} \in \mathbb{R}^{r \times q}$  and  $\mathbf{B}^{(\ell)} \in \mathbb{R}^{p \times r}$  with  $r \ll \min(p, q)$ . The fine-tuned weight is

$$\mathbf{W}_p^{(\ell)} = \mathbf{W}_0^{(\ell)} + \mathbf{B}^{(\ell)} \mathbf{A}^{(\ell)} \quad (4)$$

and only the low-rank parameters  $\mathbf{A}^{(\ell)}, \mathbf{B}^{(\ell)}$  are optimized.

Secondly, we consider cross-domain and cross-dataset robustness. In this setting, we evaluate whether fine-tuning on one downstream domain or task degrades performance on other downstream domain/tasks. Concretely, suppose we fine-tune the pre-trained model  $f_{\mathbf{W}_0}$  on a dataset  $\mathcal{D}_{\text{tr}}^{(a)}$ , obtaining the adapted parameters  $\mathbf{W}_p$ . The resulting model  $f_{\mathbf{W}_p}$  is evaluated not only on the in-domain/task test set  $\mathcal{D}_{\text{te}}^{(a)}$ , but also on out-of-domain/task test sets  $\{\mathcal{D}_{\text{te}}^{(b)} : b \neq a\}$  corresponding to other downstream datasets. **Robustness** is measured by the relative change in task-specific metric  $\mathcal{M}$  compared to the zero-shot pre-trained model  $f_{\mathbf{W}_0}$ :

$$R^{(b)} = \mathcal{M}(f_{\mathbf{W}_p}, \mathcal{D}_{\text{te}}^{(b)}) - \mathcal{M}(f_{\mathbf{W}_0}, \mathcal{D}_{\text{te}}^{(b)}). \quad (5)$$

A method is *robust* if  $R^{(b)} \geq -\epsilon$  for all  $b$ .

### 3.2 Vector-based Feature Space Adaptation

Rather than blindly updating all parameters—or indiscriminately altering the pre-trained model’s weight space—one should first understand how the downstream distribution differs from the pre-trained dataset. For example, in image classification, class semantics are largely stable across domains; discrepancies typically arise from style, background, resolution, illumination, viewpoint, and other contextual factors. These factors act as lurking variables that confound the input while leaving intrinsic class semantics unchanged.

Motivated by the EEM view of lurking variables, we propose to perform fine-tuning directly in the feature space via Vector-based Feature Space Adaptation (VeFA). Concretely, we keep  $\mathbf{W}_0^{(\ell)}$  frozen and introduce a diagonal feature-wise scaling matrix  $\Lambda_k^{(\ell)}$ , yielding the following model for the  $\ell$ -th layer:

$$\mathbf{h}^{(\ell)} = \mathbf{W}_0^{(\ell)}(\mathbf{h}^{(\ell-1)} + \mathbf{k}^{(\ell)} \odot \mathbf{h}^{(\ell-1)}) = \mathbf{W}_0^{(\ell)}(\mathbf{I} + \Lambda_k^{(\ell)})\mathbf{h}^{(\ell-1)} = \mathbf{W}_p^{(\ell)}\mathbf{h}^{(\ell-1)}$$

where  $\mathbf{I}$  is the identity matrix and  $\Lambda_k^{(\ell)} = \text{diag}(\mathbf{k}^{(\ell)})$  performs per-channel scaling of the layer input. Essentially, compared with LoRA (Fig. 2a), the updating rule of VeFA (Fig. 2b) is:

$$\mathbf{W}_p^{(\ell)} = \mathbf{W}_0^{(\ell)} + \mathbf{W}_0^{(\ell)}\Lambda_k^{(\ell)} \quad (6)$$

The vector  $\mathbf{k}$  is initialized to zero. Compared with LoRA, VeFA is substantially more parameter-efficient. Besides, since  $\text{Col}(\mathbf{W}_0\Lambda_k^{(\ell)}) \subseteq \text{Col}(\mathbf{W}_0)$ , VeFA can preserve the main representation of pre-trained weight matrix. Therefore, no intruder dimensions are introduced. In the following two sections, we demonstrate that VeFA achieves superior robustness and competitive effectiveness relative to LoRA.

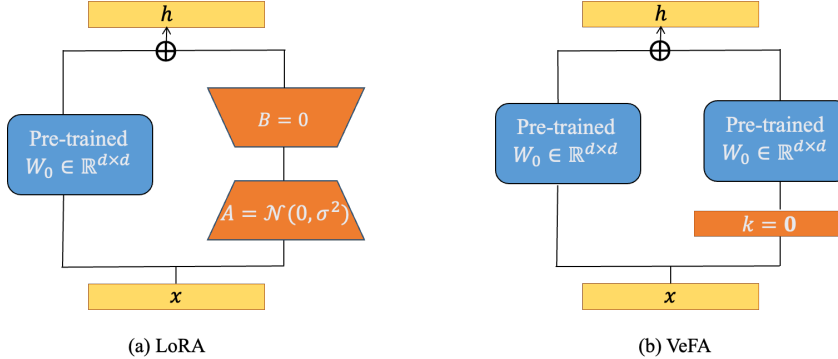


Figure 2: Schematic comparison of LoRA (left) and VeFA (right). LoRA updates the weights matrix  $\mathbf{W}$  by training the low-rank matrices  $\mathbf{A}$  and  $\mathbf{B}$ , with intermediate rank  $r$ . VeFA keeps the pre-trained  $\mathbf{W}_0$  frozen and performs adaptation at the element-wise feature level.

We use a simple one-dimensional example to illustrate the difference between **weight-space adaptation** and **feature-space adaptation**. Suppose the pre-trained model is  $y = 5x$ , and the downstream dataset consists of  $\{[0.2, 0.4], [0.6, 1.1], [1.1, 2.2], [1.6, 2.8]\}$ . Using gradient descent, we estimate  $\delta_1$  in  $y = (5 + \delta_1)x$  (weight-space adaptation) and  $\delta_2$  in  $y = 5(x + \delta_2x)$  (feature-space adaptation). The final results are shown in the Fig. 3. In weight-space fine-tuning, the model adapts by directly updating the parameters, which shifts the regression line (purple dashed) away from the pre-trained function  $f(x) = 5x$  in second sub-figure. In feature-space fine-tuning, the pre-trained model is kept frozen and adaptation is achieved by learning a lightweight transformation  $\Delta(x)$  applied to the input features (orange dashed line in first sub-figure), resulting in the orange dashed regression line in second sub-figure. The training loss curves (right) show that feature-space fine-tuning has the potential to converge faster weight-space fine-tuning (learning rate is 0.03 in this case).

## 4 Theoretical Analysis

In this section, we rigorously show that VeFA mitigates catastrophic forgetting and improves the robustness of fine-tuning. Let’s focus on the simple regression task with mean-square loss. The

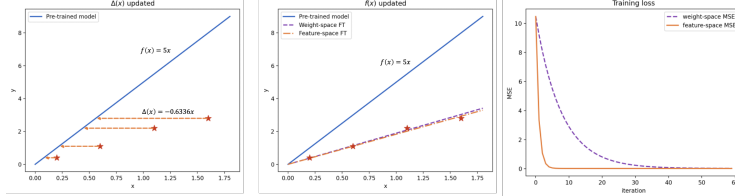


Figure 3: Comparison of weight-space fine-tuning and feature-space fine-tuning

data distribution of the downstream task is generated by the underlying true model  $\mathbf{y} = \mathbf{W}^* \mathbf{x} + \varepsilon$  with i.i.d. noise  $\varepsilon$ . Let  $\mathbf{W}_0$  and  $\mathbf{W}_p = \mathbf{W}_0 + \Delta$  be the pre-trained and fine-tuned weight matrices, respectively. In this setting, the increase in the expected loss over the data distribution (expected risk) is studied:

$$\mathcal{L}(\mathbf{W}_p | \mathbf{x}, \mathbf{y}) - \mathcal{L}(\mathbf{W}_0 | \mathbf{x}, \mathbf{y}) = \text{Tr}(\Delta \Sigma_{\mathbf{x}} \Delta^T)$$

where  $\mathbf{x}$  and  $\mathbf{y}$  follow the pre-training data distribution, and  $\Sigma_{\mathbf{x}} = \mathbb{E}(\mathbf{x}\mathbf{x}^\top)$  denotes the empirical covariance matrix of the pre-training data. This increase in the expected loss quantifies the degradation in model generalization after fine-tuning, capturing effects related to catastrophic forgetting and reduced robustness. It admits the following decomposition as  $\Delta = P_{\mathcal{S}_0} \Delta + P_{\mathcal{S}_0}^\perp \Delta$ :

$$\begin{aligned} \text{Tr}(\Delta \Sigma_{\mathbf{x}} \Delta^T) &= \text{Tr}(P_{\mathcal{S}_0} \Delta \Sigma_{\mathbf{x}} \Delta^T P_{\mathcal{S}_0}^T) + \text{Tr}(P_{\mathcal{S}_0}^\perp \Delta \Sigma_{\mathbf{x}} \Delta^T P_{\mathcal{S}_0}^{\perp T}) + 2\text{Tr}(P_{\mathcal{S}_0}^\perp \Delta \Sigma_{\mathbf{x}} \Delta^T P_{\mathcal{S}_0}^T) \\ &= \text{Tr}(P_{\mathcal{S}_0} \Delta \Sigma_{\mathbf{x}} \Delta^T P_{\mathcal{S}_0}^T) + \text{Tr}(P_{\mathcal{S}_0}^\perp \Delta \Sigma_{\mathbf{x}} \Delta^T P_{\mathcal{S}_0}^{\perp T}). \end{aligned}$$

The cross term is canceled as the result of cyclic property of trace and  $P_{\mathcal{S}_0} P_{\mathcal{S}_0}^\perp = \mathbf{0}$ . We can see that both terms in the decomposition are non-negative, which is reasonable since  $\mathbf{W}_0$  is the best estimator for the pre-training data. The first term of the loss corresponds to transformations within the column space of  $\mathbf{W}_0$ , while the second term captures the forgetting or harmful changes introduced by intruder dimensions. For VeFA, the second term (which corresponds to the intruder dimensions) is zero; therefore, it does not suffer from the intruder-dimension-induced forgetting that arises in LoRA. In contrast, when intruder dimensions are introduced, this term becomes strictly positive and admits an explicit lower bound, quantifying the additional forgetting purely attributable to these intruder directions. Proof of this proposition can be seen in Appendix C.1.

**Proposition 1.** *If  $P_{\mathcal{S}_0}^\perp \Delta \neq \mathbf{0}$ , the increase in expected loss attributable to the intruder dimensions is bounded from below by:*

$$\text{Tr}(P_{\mathcal{S}_0}^\perp \Delta \Sigma_{\mathbf{x}} \Delta^T P_{\mathcal{S}_0}^{\perp T}) \geq \sigma_{\min}(\Sigma_{\mathbf{x}}) \left[ \sqrt{(1 - \varepsilon)r_p \sigma_{p,r_p}^2} - \sqrt{1 - \alpha} \|\mathbf{W}_0\|_F \right]^2.$$

For VeFA, the first loss term can be bounded by Proposition 2; notably, the bound depends only on the maximum absolute entry of the diagonal vector  $\mathbf{k}$ , so enforcing  $\|\mathbf{k}\|_\infty \leq \gamma$  yields a global bound on the total forgetting under VeFA. In the next section we empirically show across all tasks that  $\max_j |k_j|$  of the fine-tuned matrices remains small even without an explicit constraint (see in Appendix D.1). This is also intuitively reasonable: since VeFA only rescales feature dimensions, very large  $|k_j|$  would severely distort the pre-trained feature magnitudes and be strongly penalized by the fine-tuning loss, so gradient-based optimization naturally keeps these scaling factors small.

**Proposition 2.** *Assume that  $\Sigma_{\mathbf{x}}$  and  $\|\mathbf{W}_0\|_F$  are bounded. For VeFA, the in-subspace term satisfies*

$$\text{Tr}(P_{\mathcal{S}_0} \Delta \Sigma_{\mathbf{x}} \Delta^T P_{\mathcal{S}_0}^T) \leq \|\Sigma_{\mathbf{x}}\|_2 \|\mathbf{W}_0\|_F^2 (\max_j |k_j|)^2.$$

In summary, VeFA introduces no intruder dimensions and therefore avoids the associated intruder-induced forgetting. Within the original main column space of  $\mathbf{W}_0$ , the transformation loss is tightly bounded and controlled by the small feature-wise scaling factors  $\mathbf{k}$ , so the overall forgetting under VeFA remains bounded. Consequently, VeFA exhibits substantially reduced catastrophic forgetting and correspondingly stronger robustness compared to weight-space fine-tuning methods such as LoRA.

## 5 Experiment

### 5.1 Experiment setup

**Pre-trained models and downstream tasks.** To demonstrate the effectiveness and rationality of our feature-space based fine-tuning method, we fine-tune four different pre-trained model on corresponding downstream datasets.

1. Image Classification (ResNet-18: MNIST  $\rightarrow$  USPS [24, 25]). This dataset serves as a toy example to illustrate the effectiveness of feature-space adaptation based on EEM. We fine-tune a ResNet-18 model pre-trained on MNIST to the USPS dataset. In the downstream setting, only a subset of USPS classes is available during fine-tuning, while evaluation is conducted on both seen and unseen classes. This setup directly measures the first robustness metric  $R_1$ .
2. Image Classification (CLIP across seven datasets [2, 26]). We fine-tune CLIP (Contrastive Language–Image Pre-training, ViT-B/16 backbone) on seven diverse image classification datasets. In each case, the model is fine-tuned on one dataset and then evaluated on the others. By comparing fine-tuned performance with CLIP’s zero-shot baseline, we assess the second robustness metric  $R_1$ , i.e., the cross-dataset robustness of different fine-tuning strategies.
3. Natural Language Understanding (RoBERTa on GLUE[27, 28]). We evaluate RoBERTa (Robustly Optimized BERT Pre-training) on the GLUE benchmark. Since fine-tuning requires the addition of task-specific classification heads, robustness comparisons may be confounded. Therefore, GLUE is primarily used to validate the feasibility and effectiveness of LoRFA and VeFA in NLU tasks, rather than as a robustness benchmark.
4. Natural Language Generation (GPT-2 on E2E[3, 29]). We fine-tune GPT-2 on the E2E NLG benchmark and subsequently evaluate its zero-shot transfer to two additional benchmarks, DART and WebNLG. The comparison with zero-shot GPT-2 serves to quantify R2 in the generative setting, using standard NLG evaluation metrics.

**Experiment Platform.** All our experiments were conducted on a 40GB NVIDIA A100 GPU.

### 5.2 Fine-tuning CLIP for Image Classification

We follows the setting of previous work [30, 26]. We evaluate on seven datasets spanning diverse visual domains—satellite imagery (EuroSAT [31]), food (Food101 [32]), pet breeds (OxfordPets [33]), flowers (Flower102 [34]), generic objects (Caltech101 [35]), textures (DTD [36]), and human actions (UCF101 [37]). Together, these datasets provide a comprehensive benchmark for visual classification.

We compare our simplest model, VeFA, against LoRA (rank  $r = 2$ ) in terms of few-shot learning performance and cross-dataset robustness. In few-shot learning, a “shot” refers to the number of labeled training examples provided per class. We conduct experiments under 1-shot, 4-shot, and 16-shot learning settings, and the results are presented in Tab 1. With only 25% of LoRA’s trainable parameters, VeFA outperforms on average in the 1-shot and 4-shot settings, achieves comparable results in the 16-shot setting, and consistently demonstrates superior robustness across all seven datasets. These results highlight the advantage of feature-space adaptation, which enables effective knowledge transfer while better preserving pre-trained representations.

### 5.3 Natural Language Understanding

We evaluate on the General Language Understanding Evaluation (GLUE) benchmark [28] using RoBERTa-base and RoBERTa-large [27]. We compare our simplest variant, VeFA, against LoRA. Our experiment broadly follows setting in LoRA [9]: we adapt the query and value projection matrices in each self-attention block and fully train the task-specific classification head. Unlike [9], which employs an auxiliary hyperparameter  $\alpha$  to rescale gradients in adapted layers, we use separate learning rates for (i) the classification head and (ii) the adapted layers. Learning rates and training epochs are chosen via hyperparameter tuning; full settings appear in Appendix B). We use batch size 64 for RoBERTa-base and 32 for RoBERTa-large, with maximum sequence lengths of 512 and 256, respectively.

Table 1: Performance comparison between LoRA and VeFA across different datasets under zero-shot, 1-shot, 4-shot, 16-shot fine-tuning, and robustness settings. The visual backbone is ViT-B/16. Best results are in **bold**.

| Shots           | Method | Caltech101  | Food101     | Oxford Pets | Oxford Flowers | EuroSAT     | DTD         | UCF101      |
|-----------------|--------|-------------|-------------|-------------|----------------|-------------|-------------|-------------|
| 0               | CLIP   | 92.9        | 85.2        | 89.1        | 67.3           | 42.2        | 43.6        | 65.1        |
| 1               | LoRA   | 93.7        | 84.3        | 92.3        | 82.3           | 72.3        | 54.3        | <b>76.3</b> |
|                 | VeFA   | <b>94.1</b> | <b>86.3</b> | <b>93.3</b> | <b>84.3</b>    | <b>73.3</b> | <b>55.0</b> | 74.2        |
| 4               | LoRA   | 95.2        | 82.7        | 91.0        | <b>93.7</b>    | 84.9        | 63.8        | <b>81.1</b> |
|                 | VeFA   | <b>95.6</b> | <b>86.0</b> | <b>93.4</b> | 93.0           | <b>87.1</b> | <b>65.7</b> | 80.2        |
| 16              | LoRA   | 96.4        | 84.2        | 92.4        | <b>98.0</b>    | <b>92.1</b> | 72.0        | <b>86.7</b> |
|                 | LoRFA  | 96.3        | 87.6        | <b>94.5</b> | 97.7           | 91.4        | 72.3        | 86.4        |
|                 | VeFA   | 96.4        | <b>87.8</b> | 94.4        | 97.5           | 91.3        | <b>72.5</b> | 86.4        |
| $\bar{R}^{(b)}$ | LoRA   | -2.4        | -3.8        | -2.8        | -4.4           | -14.1       | -3.0        | -1.1        |
|                 | VeFA   | <b>+0.2</b> | <b>-0.6</b> | <b>-0.4</b> | <b>+0.4</b>    | <b>-2.3</b> | <b>+2.0</b> | <b>+0.3</b> |

For initialization, because our feature-space method does not rely on random low-rank matrices (as in LoRA/VeRA), the diagonal scaling parameters (denoted  $\Lambda_b^{(\ell)}$ ) are initialized to zero; consequently, we only report results with random seed = 0 for reproducibility. Finally, since fine-tuning introduces task-specific classification heads that can confound robustness comparisons, GLUE is used here primarily to establish the feasibility of feature-space adaptation on natural language tasks rather than to get robustness claims.

The experimental results are presented in Tab. 2. VeFA achieves performance comparable to LoRA across both models, while requiring an order of magnitude fewer parameters. The experiment also validates the effectiveness of feature-space adaptation to achieve fine-tuning for natural languages tasks.

Table 2: Performance on GLUE with different fine-tuning methods. We report Matthews correlation for CoLA, Pearson correlation for STS-B, and accuracy for all other tasks; in every case, higher is better. Results for all methods except VeFA are taken from prior work ([9, 38]). With an order of magnitude fewer trainable parameters, VeFA achieves performance on par with LoRA.

|       | Method | # Params      | SST-2          | MRPC           | CoLA           | QNLI           | RTE            | STSB           | AVG  |
|-------|--------|---------------|----------------|----------------|----------------|----------------|----------------|----------------|------|
| Base  | FT     | 125M          | 94.8           | 90.2           | 63.6           | 92.8           | 78.7           | 91.2           | 85.2 |
|       | BitFit | 0.1M          | 93.7           | 92.7           | 62.0           | 91.8           | 81.5           | 90.8           | 85.4 |
|       | Adpt   | 0.3M          | 94.2 $\pm$ 0.1 | 88.5 $\pm$ 1.1 | 60.8 $\pm$ 0.4 | 93.1 $\pm$ 0.1 | 71.5 $\pm$ 2.7 | 89.7 $\pm$ 0.3 | 83.0 |
|       | LoRA   | 0.3M          | 95.1 $\pm$ 0.2 | 89.7 $\pm$ 0.7 | 63.4 $\pm$ 1.2 | 93.3 $\pm$ 0.3 | 86.6 $\pm$ 0.7 | 91.5 $\pm$ 0.2 | 86.6 |
|       | VeRA   | 0.043M        | 94.6 $\pm$ 0.1 | 89.5 $\pm$ 0.5 | 65.6 $\pm$ 0.8 | 91.8 $\pm$ 0.2 | 78.7 $\pm$ 0.7 | 90.7 $\pm$ 0.2 | 85.2 |
|       | VeFA   | <b>0.018M</b> | 94.1           | 89.7           | 63.3           | 91.7           | 83.0           | 90.7           | 85.4 |
| Large | LoRA   | 0.8M          | 96.2 $\pm$ 0.5 | 90.2 $\pm$ 1.0 | 68.2 $\pm$ 1.9 | 94.8 $\pm$ 0.3 | 85.2 $\pm$ 1.1 | 92.3 $\pm$ 0.5 | 87.8 |
|       | VeRA   | 0.061M        | 96.1 $\pm$ 0.1 | 90.9 $\pm$ 0.7 | 68.0 $\pm$ 0.8 | 94.4 $\pm$ 0.2 | 85.9 $\pm$ 0.7 | 91.7 $\pm$ 0.8 | 87.8 |
|       | VeFA   | <b>0.049M</b> | 95.8           | 90.4           | 68.0           | 94.1           | 87.4           | 91.4           | 87.8 |

#### 5.4 Natural Language Generation

We evaluate on the E2E benchmark [29], following the experimental protocol of setting for LoRA [9]. We fine-tune GPT-2 Medium and Large [3]. For LoRA, we use the same implementation and hyperparameters from the original paper [9]. For feature space adaptation, we still use our simplest variant, VeFA. A complete list of hyperparameters is provided in Appendix B.

The E2E benchmark contains a single task: given a meaning representation, generate natural-language descriptions. We evaluate with five metrics—BLEU, NIST, MET, ROUGE-L, and CIDEr—to comprehensively assess generation quality. We report the results from the final epoch. As shown in Tab. 3, VeFA outperforms LoRA for both GPT-2 Medium and GPT-2 Large models.

Table 3: Performance comparison of LoRA and VeFA on GPT-2 Medium and GPT-2 Large using standard NLG evaluation metrics.

|        | Method | BLEU  | NIST   | MET   | ROUGE-L | CIDEr  |
|--------|--------|-------|--------|-------|---------|--------|
| Medium | LoRA   | 67.04 | 8.5753 | 45.92 | 68.74   | 2.3507 |
|        | VeFA   | 66.42 | 8.5852 | 44.40 | 66.46   | 2.2134 |
| Large  | LoRA   | 67.38 | 8.6293 | 45.98 | 68.82   | 2.3320 |
|        | VeFA   | 67.62 | 8.5956 | 46.04 | 68.77   | 2.3858 |

## 6 Conclusion

This work proposes a novel feature space fine-tuning framework based on effect equivalence modeling (EEM), providing an alternative to conventional weight space-updating strategies. A central insight is that domain discrepancies often arise from lurking variables rather than intrinsic changes in the input–output mapping. By adapting in the feature space—learning input transformations or lightweight layer-wise modifications—the proposed method compensates for these confounding effects while largely preserving the original parameters of the pre-trained model.

Our empirical results across vision and language tasks demonstrate that feature-space adaptation (LoRFA and VeFA) can achieve accuracy comparable to or exceeding weight-space methods such as LoRA, despite requiring significantly fewer trainable parameters. In particular, VeFA attains on-par performance with magnitude less of LoRA’s parameter budget, and consistently shows stronger robustness across datasets. These findings highlight the practical advantages of feature-space fine-tuning for balancing efficiency, robustness, and generalization.

Nevertheless, the effectiveness of feature-space adaptation depends on the quality of the pre-trained model and the severity of the domain shift: when generalization capacity is limited or the downstream distribution diverges substantially, learned transformations may not fully recover alignment. Future work should therefore investigate hybrid strategies that combine feature-space adaptation with selective weight updating, as well as methods for adaptively choosing the degree of intervention at different layers.

Overall, this study contributes to the development of robust, interpretable, and parameter-efficient fine-tuning approaches, and provides a foundation for advancing transformation-based model adaptation in both vision and language domains.

## References

- [1] R. Bommasani, D. A. Hudson, E. Adeli, R. Altman, S. Arora, S. von Arx, M. S. Bernstein, J. Bohg, A. Bosselut, E. Brunskill, et al., On the opportunities and risks of foundation models, arXiv preprint arXiv:2108.07258 (2021).
- [2] A. Radford, J. W. Kim, C. Hallacy, A. Ramesh, G. Goh, S. Agarwal, G. Sastry, A. Askell, P. Mishkin, J. Clark, et al., Learning transferable visual models from natural language supervision, in: International conference on machine learning, PMLR, 2021, pp. 8748–8763.
- [3] A. Radford, J. Wu, R. Child, D. Luan, D. Amodei, I. Sutskever, et al., Language models are unsupervised multitask learners, OpenAI blog 1 (8) (2019) 9.
- [4] C. Gardent, A. Shimorina, S. Narayan, L. Perez-Beltrachini, The webnlg challenge: Generating text from rdf data, in: 10th International Conference on Natural Language Generation, ACL Anthology, 2017, pp. 124–133.
- [5] J. Devlin, M.-W. Chang, K. Lee, K. Toutanova, Bert: Pre-training of deep bidirectional transformers for language understanding, in: Proceedings of the 2019 conference of the North American chapter of the association for computational linguistics: human language technologies, volume 1 (long and short papers), 2019, pp. 4171–4186.
- [6] A. Kumar, A. Raghunathan, R. Jones, T. Ma, P. Liang, Fine-tuning can distort pretrained features and underperform out-of-distribution, arXiv preprint arXiv:2202.10054 (2022).
- [7] E. B. Zaken, S. Ravfogel, Y. Goldberg, Bitfit: Simple parameter-efficient fine-tuning for transformer-based masked language-models, arXiv preprint arXiv:2106.10199 (2021).
- [8] N. Houlsby, A. Giurgiu, S. Jastrzebski, B. Morrone, Q. De Laroussilhe, A. Gesmundo, M. Attariyan, S. Gelly, Parameter-efficient transfer learning for nlp, in: International conference on machine learning, PMLR, 2019, pp. 2790–2799.
- [9] E. J. Hu, Y. Shen, P. Wallis, Z. Allen-Zhu, Y. Li, S. Wang, L. Wang, W. Chen, et al., Lora: Low-rank adaptation of large language models., ICLR 1 (2) (2022) 3.
- [10] R. Shuttleworth, J. Andreas, A. Torralba, P. Sharma, Lora vs full fine-tuning: An illusion of equivalence, arXiv preprint arXiv:2410.21228 (2024).
- [11] R. M. French, Catastrophic forgetting in connectionist networks, Trends in cognitive sciences 3 (4) (1999) 128–135.
- [12] J. Kirkpatrick, R. Pascanu, N. Rabinowitz, J. Veness, G. Desjardins, A. A. Rusu, K. Milan, J. Quan, T. Ramalho, A. Grabska-Barwinska, et al., Overcoming catastrophic forgetting in neural networks, Proceedings of the national academy of sciences 114 (13) (2017) 3521–3526.
- [13] R. Kemker, M. McClure, A. Abitino, T. Hayes, C. Kanan, Measuring catastrophic forgetting in neural networks, in: Proceedings of the AAAI conference on artificial intelligence, Vol. 32, 2018.
- [14] J. Serra, D. Suris, M. Miron, A. Karatzoglou, Overcoming catastrophic forgetting with hard attention to the task, in: International conference on machine learning, PMLR, 2018, pp. 4548–4557.
- [15] M. Wortsman, G. Ilharco, J. W. Kim, M. Li, S. Kornblith, R. Roelofs, R. G. Lopes, H. Hajishirzi, A. Farhadi, H. Namkoong, et al., Robust fine-tuning of zero-shot models, in: Proceedings of the IEEE/CVF conference on computer vision and pattern recognition, 2022, pp. 7959–7971.
- [16] G. E. Box, Use and abuse of regression, Technometrics 8 (4) (1966) 625–629.
- [17] B. L. Joiner, Lurking variables: Some examples, The American Statistician 35 (4) (1981) 227–233.
- [18] W. G. Hunter, J. J. Crowley, Hazardous substances, the environment and public health: a statistical overview., Environmental health perspectives 32 (1979) 241–254.
- [19] Z. Mai, A. Chowdhury, P. Zhang, C.-H. Tu, H.-Y. Chen, V. Pahuja, T. Berger-Wolf, S. Gao, C. Stewart, Y. Su, et al., Fine-tuning is fine, if calibrated, Advances in Neural Information Processing Systems 37 (2024) 136084–136119.
- [20] T. Brown, B. Mann, N. Ryder, M. Subbiah, J. D. Kaplan, P. Dhariwal, A. Neelakantan, P. Shyam, G. Sastry, A. Askell, et al., Language models are few-shot learners, Advances in neural information processing systems 33 (2020) 1877–1901.

[21] Q. Huang, J. Zhang, A. Sabbaghi, T. Dasgupta, Optimal offline compensation of shape shrinkage for three-dimensional printing processes, *Iie transactions* 47 (5) (2015) 431–441.

[22] A. Sabbaghi, Q. Huang, Model transfer across additive manufacturing processes via mean effect equivalence of lurking variables, *The Annals of Applied Statistics* 12 (4) (2018) 2409–2429.

[23] A. Abadie, J. Gardeazabal, The economic costs of conflict: A case study of the basque country, *American economic review* 93 (1) (2003) 113–132.

[24] Y. LeCun, L. Bottou, Y. Bengio, P. Haffner, Gradient-based learning applied to document recognition, *Proceedings of the IEEE* 86 (11) (1998) 2278–2324.

[25] Y. LeCun, B. Boser, J. S. Denker, D. Henderson, R. E. Howard, W. Hubbard, L. D. Jackel, Backpropagation applied to handwritten zip code recognition, *Neural computation* 1 (4) (1989) 541–551.

[26] M. Zanella, I. Ben Ayed, Low-rank few-shot adaptation of vision-language models, in: *Proceedings of the IEEE/CVF Conference on Computer Vision and Pattern Recognition*, 2024, pp. 1593–1603.

[27] Y. Liu, M. Ott, N. Goyal, J. Du, M. Joshi, D. Chen, O. Levy, M. Lewis, L. Zettlemoyer, V. Stoyanov, Roberta: A robustly optimized bert pretraining approach, *arXiv preprint arXiv:1907.11692* (2019).

[28] A. Wang, A. Singh, J. Michael, F. Hill, O. Levy, S. R. Bowman, Glue: A multi-task benchmark and analysis platform for natural language understanding, *arXiv preprint arXiv:1804.07461* (2018).

[29] J. Novikova, O. Dušek, V. Rieser, The e2e dataset: New challenges for end-to-end generation, *arXiv preprint arXiv:1706.09254* (2017).

[30] K. Zhou, J. Yang, C. C. Loy, Z. Liu, Learning to prompt for vision-language models, *International Journal of Computer Vision* 130 (9) (2022) 2337–2348.

[31] P. Helber, B. Bischke, A. Dengel, D. Borth, Eurosat: A novel dataset and deep learning benchmark for land use and land cover classification, *IEEE Journal of Selected Topics in Applied Earth Observations and Remote Sensing* 12 (7) (2019) 2217–2226.

[32] L. Bossard, M. Guillaumin, L. Van Gool, Food-101–mining discriminative components with random forests, in: *European conference on computer vision*, Springer, 2014, pp. 446–461.

[33] O. M. Parkhi, A. Vedaldi, A. Zisserman, C. Jawahar, Cats and dogs, in: *2012 IEEE conference on computer vision and pattern recognition*, IEEE, 2012, pp. 3498–3505.

[34] M.-E. Nilsback, A. Zisserman, Automated flower classification over a large number of classes, in: *2008 Sixth Indian conference on computer vision, graphics & image processing*, IEEE, 2008, pp. 722–729.

[35] L. Fei-Fei, R. Fergus, P. Perona, Learning generative visual models from few training examples: An incremental bayesian approach tested on 101 object categories, in: *2004 conference on computer vision and pattern recognition workshop*, IEEE, 2004, pp. 178–178.

[36] M. Cimpoi, S. Maji, I. Kokkinos, S. Mohamed, A. Vedaldi, Describing textures in the wild, in: *Proceedings of the IEEE conference on computer vision and pattern recognition*, 2014, pp. 3606–3613.

[37] K. Soomro, A. R. Zamir, M. Shah, Ucf101: A dataset of 101 human actions classes from videos in the wild, *arXiv preprint arXiv:1212.0402* (2012).

[38] D. J. Kopitzko, T. Blankevoort, Y. M. Asano, Vera: Vector-based random matrix adaptation, *arXiv preprint arXiv:2310.11454* (2023).

[39] C. Lee, K. Cho, W. Kang, Mixout: Effective regularization to finetune large-scale pretrained language models, in: *International Conference on Learning Representations*.

[40] S. Han, J. Pool, J. Tran, W. Dally, Learning both weights and connections for efficient neural network, *Advances in neural information processing systems* 28 (2015).

[41] J. Lee, S. Park, S. Mo, S. Ahn, J. Shin, Layer-adaptive sparsity for the magnitude-based pruning, *arXiv preprint arXiv:2010.07611* (2020).

[42] F. Lagunas, E. Charlaix, V. Sanh, A. M. Rush, Block pruning for faster transformers, *arXiv preprint arXiv:2109.04838* (2021).

[43] J. Pfeiffer, A. Rücklé, C. Poth, A. Kamath, I. Vulić, S. Ruder, K. Cho, I. Gurevych, Adapterhub: A framework for adapting transformers, *arXiv preprint arXiv:2007.07779* (2020).

[44] A. Rücklé, G. Geigle, M. Glockner, T. Beck, J. Pfeiffer, N. Reimers, I. Gurevych, Adapterdrop: On the efficiency of adapters in transformers, arXiv preprint arXiv:2010.11918 (2020).

[45] R. Karimi Mahabadi, J. Henderson, S. Ruder, Compacter: Efficient low-rank hypercomplex adapter layers, Advances in neural information processing systems 34 (2021) 1022–1035.

[46] A. Panahi, S. Saeedi, T. Arodz, Shapeshifter: a parameter-efficient transformer using factorized reshaped matrices, Advances in Neural Information Processing Systems 34 (2021) 1337–1350.

[47] A. Mallya, D. Davis, S. Lazebnik, Piggyback: Adapting a single network to multiple tasks by learning to mask weights, in: Proceedings of the European conference on computer vision (ECCV), 2018, pp. 67–82.

[48] V. Sanh, T. Wolf, A. Rush, Movement pruning: Adaptive sparsity by fine-tuning, Advances in neural information processing systems 33 (2020) 20378–20389.

[49] R. Xu, F. Luo, Z. Zhang, C. Tan, B. Chang, S. Huang, F. Huang, Raise a child in large language model: Towards effective and generalizable fine-tuning, arXiv preprint arXiv:2109.05687 (2021).

[50] H. Mostafa, X. Wang, Parameter efficient training of deep convolutional neural networks by dynamic sparse reparameterization, in: International Conference on Machine Learning, PMLR, 2019, pp. 4646–4655.

[51] J.-Y. Zhu, T. Park, P. Isola, A. A. Efros, Unpaired image-to-image translation using cycle-consistent adversarial networks, in: Proceedings of the IEEE international conference on computer vision, 2017, pp. 2223–2232.

[52] Y. Ganin, E. Ustinova, H. Ajakan, P. Germain, H. Larochelle, F. Laviolette, M. March, V. Lempitsky, Domain-adversarial training of neural networks, Journal of machine learning research 17 (59) (2016) 1–35.

[53] J. Liang, D. Hu, J. Feng, Do we really need to access the source data? source hypothesis transfer for unsupervised domain adaptation, in: International conference on machine learning, PMLR, 2020, pp. 6028–6039.

[54] S. Motiian, M. Piccirilli, D. A. Adjeroh, G. Doretto, Unified deep supervised domain adaptation and generalization, in: Proceedings of the IEEE international conference on computer vision, 2017, pp. 5715–5725.

## A Related Work

**Parameter Efficient Fine Tuning (PEFT).** PEFT aims to selectively fine-tune a small subset of parameters or incorporate lightweight trainable modules—a task that is inherently NP-hard. Existing PEFT approaches can be categorized into random approaches, rule-based approaches, and projection-based approaches based on how they choose which parameters to tune. **Randomized approaches**, such as the Random and Mixout models [39], select parameters for fine-tuning without relying on task-specific data information. **Rule-based approaches** such as BitFit ([7]), MagPruning ([40–42]), Adapter ([8, 43, 44]), and LoRA ([9, 45, 46]) determine which parameters to fine-tune based on pre-defined heuristics. These methods incorporate prior knowledge to identify potentially important components in the model, thereby addressing some of the limitations of randomized approaches. However, the parameter selection process remains independent of the specific downstream data. Among rule-based PEFT methods, **LoRA** has become a de facto baseline due to its simplicity, hardware efficiency, and strong empirical performance across modalities. In our experiments, LoRA also serves as the primary baseline for comparison. **Projection-based approaches**, such as DiffPruning [47, 48, 42] and ChildPruning ([49, 50]), aim to leverage task-specific data to guide the selection of tunable parameters in a pre-trained model. Our approach also falls under the category of PEFT; however, it differs fundamentally from prior PEFT methods in that we perform fine-tuning in the feature space rather than the weight space. Unlike weight-based methods, our fine-tuning does not alter the column space of  $W_0$ , thereby preserving pre-training knowledge more effectively throughout adaptation. This design is particularly advantageous when fine-tuning large-scale models (e.g., the 175-billion parameter GPT-3), where maintaining the integrity of pre-trained representations significantly improves robustness.

**Domain Adaptation.** Although our method explicitly models and compensates for domain discrepancy, it fundamentally differs from existing domain adaptation (DA) approaches [51–54]. DA methods generally rely on joint access to source and target data and seek to learn a domain-invariant representation by optimizing the feature extractor accordingly. In contrast, our problem setting assumes that source domain data is unavailable and needs to revise the pre-trained model to adapt to the downstream data. We perform feature-space transformation at the layer level, but the focus ultimately remains on parameter adaptation. Moreover, the domain discrepancy in our problem setting is substantially greater than that typically encountered in standard domain adaptation tasks. These distinctions position our work closer to fine-tuning methodologies rather than DA frameworks.

## B Hyperparameter

Table 4: Hyper-parameter settings for RoBERTa-Base and RoBERTa-Large on GLUE benchmark tasks.

| Model        | Hyper-Parameters     | SST-2  | MRPC | CoLA | QNLI | RTE  | STS-B |
|--------------|----------------------|--------|------|------|------|------|-------|
| Optimizer    |                      | AdamW  |      |      |      |      |       |
| Warmup Ratio |                      | 0.06   |      |      |      |      |       |
| LR Schedule  |                      | Linear |      |      |      |      |       |
| Base         | Epochs               | 60     | 30   | 80   | 25   | 80   | 50    |
|              | Learning Rate (VeFA) | 1E-2   | 1E-2 | 1E-2 | 1E-2 | 4E-3 | 4E-3  |
|              | Weight Decay (VeFA)  | 0.05   | 0    | 0    | 0.01 | 0.1  | 0.1   |
|              | Learning Rate (Head) | 4E-3   | 4E-3 | 1E-2 | 4E-3 | 4E-3 | 4E-3  |
|              | Weight Decay (Head)  | 0.05   | 0.01 | 0.01 | 0.05 | 0.1  | 0.1   |
|              | Max Seq. Len.        | 512    |      |      |      |      |       |
|              | Batch Size           | 64     |      |      |      |      |       |
|              | Epochs               | 40     | 20   | 20   | 25   | 20   | 20    |
| Large        | Learning Rate (VeFA) | 1E-2   | 2E-2 | 1E-2 | 1E-2 | 2E-2 | 4E-3  |
|              | Weight Decay (VeFA)  | 0.1    | 0.1  | 0    | 0.01 | 0.1  | 0.1   |
|              | Learning Rate (Head) | 6E-3   | 4E-3 | 4E-3 | 4E-4 | 4E-3 | 4E-3  |
|              | Weight Decay (Head)  | 0.1    | 0.1  | 0.01 | 0.01 | 0.1  | 0.1   |
|              | Max Seq. Len.        | 256    |      |      |      |      |       |
|              | Batch Size           | 32     |      |      |      |      |       |

Table 5: Hyperparameter configurations for VeFA on the E2E benchmark, for GPT-2 Medium and Large models.

| Hyperparameter         | Medium | Large |
|------------------------|--------|-------|
| # GPUs                 | 1      | 1     |
| Optimizer              | AdamW  |       |
| Learning Rate Schedule | Linear |       |
| Weight Decay           | 0.01   |       |
| Batch Size             | 8      |       |
| Epochs                 | 5      |       |
| Warmup Steps           | 500    |       |
| Label Smooth           | 0.1    |       |
| Learning Rate          | 3E-2   | 2E-2  |

## C Proof of Theoretical Analysis

### C.1 Proof of Proposition 1

Since  $P_{S_0}^\perp$  is the projection operator admitting  $P_{S_0}^\perp = P_{S_0}^\perp P_{S_0}^\perp$ , the above inequality can be further written as:

$$\begin{aligned}
\text{Tr} \left( P_{S_0}^\perp \Delta \Sigma_{\mathbf{x}} \Delta^T P_{S_0}^{\perp T} \right) &= \sum_i \sigma_i(\Sigma_{\mathbf{x}}) \cdot \left\| \left[ P_{S_0}^\perp \Delta Q \right]_{\cdot, i} \right\|_2^2 \\
&\geq \sigma_{\min}(\Sigma_{\mathbf{x}}) \sum_i \left\| \left[ P_{S_0}^\perp \Delta Q \right]_{\cdot, i} \right\|_2^2 \\
&= \sigma_{\min}(\Sigma_{\mathbf{x}}) \sum_i \left\| P_{S_0}^\perp \Delta Q \right\|_F^2 \\
&= \sigma_{\min}(\Sigma_{\mathbf{x}}) \left\| P_{S_0}^\perp \Delta \right\|_F^2,
\end{aligned}$$

in which  $Q$  is unitary/conjugate matrix in the SVD of  $\Sigma_{\mathbf{x}}$  (or equivalently orthogonal diagonalization for such symmetric matrix), and thus  $Q$  is orthogonal and is canceled in the Frobenius norm.

If we write the weight change  $\Delta$  as the difference between  $\mathbf{W}_p$  and  $\mathbf{W}_0$ , the F-norm component admits:

$$\left\| P_{S_0}^\perp \Delta \right\|_F \geq \left\| P_{S_0}^\perp \mathbf{W}_p \right\|_F - \left\| P_{S_0}^\perp \mathbf{W}_0 \right\|_F.$$

in which:

$$\begin{aligned}
P_{S_0}^\perp \mathbf{W}_p &= P_{S_0}^\perp \sum_{i=1}^r \sigma_{p,i} \mathbf{u}_{p,i} \mathbf{v}_{p,i}^T \\
&= \sum_{i=1}^r \sigma_{p,i} \left( P_{S_0}^\perp \mathbf{u}_{p,i} \right) \mathbf{v}_{p,i}^T
\end{aligned}$$

and further:

$$\begin{aligned}
\left\| P_{S_0}^\perp \mathbf{W}_p \right\|_F^2 &= \text{Tr} \left( P_{S_0}^\perp \mathbf{W}_p (P_{S_0}^\perp \mathbf{W}_p)^T \right) \\
&= \sum_{i=1}^r \sigma_{p,i}^2 \left\| P_{S_0}^\perp \mathbf{u}_{p,i} \right\|_2^2
\end{aligned}$$

From the definition of intruder dimension above, it is straightforward that the projection of vector  $\mathbf{u}_{p,i}$  onto the complement of  $S_0$  will have an upper bound  $1 - \varepsilon$ , and therefore:

$$\left\| P_{S_0}^\perp \mathbf{W}_p \right\|_F^2 > (1 - \varepsilon) \sum_{i=1}^r \sigma_{p,i}^2 \geq (1 - \varepsilon) r_p \sigma_{p,r_p}^2.$$

On the other hand,  $\left\| P_{S_0}^\perp \mathbf{W}_0 \right\|_F^2 = \sum_{i=r_0+1}^r \sigma_{0,i}^2 \left\| P_{S_0}^\perp \mathbf{u}_{0,i} \right\|_2^2 = \sum_{i=r_0+1}^r \sigma_{0,i}^2$  measures the residual portion of spectral power:

$$\left\| P_{S_0}^\perp \mathbf{W}_0 \right\|_F^2 \leq (1 - \alpha) \left\| \mathbf{W}_0 \right\|_F^2.$$

Combining the two parts together, we can then derive the bound:

$$\begin{aligned}
\Delta \mathcal{L} &\geq \sigma_{\min}(\Sigma_{\mathbf{x}}) \left\| P_{S_0}^\perp \Delta \right\|_F^2 \\
&\geq \sigma_{\min}(\Sigma_{\mathbf{x}}) \left[ \sqrt{(1 - \varepsilon) r_p \sigma_{p,r_p}^2} - \sqrt{1 - \alpha} \left\| \mathbf{W}_0 \right\|_F \right]_+^2
\end{aligned}$$

## D Additional Numerical Experiments

### D.1 Maximum VeFA Scaling Coefficient

Tables 6, 7 and 8 report the maximum VeFA scaling coefficient  $\|\mathbf{k}\|_\infty$  across all layers for each task and backbone. For image classification (Table 6), all datasets yield  $\|\mathbf{k}\|_\infty \leq 1.9$ , indicating only mild rescaling of feature dimensions. On GLUE NLU tasks (Table 7), both RoBERTa-Base and RoBERTa-Large exhibit similarly small scaling factors, mostly in the range 1.4–3.9. For NLG with GPT-2 (Table 8), the maximal values remain below 6.2. Overall, these results confirm that VeFA operates with relatively small feature-wise scalings in practice, which is consistent with our theoretical analysis that the forgetting under VeFA is bounded and controlled by  $\|\mathbf{k}\|_\infty$ .

Table 6: Maximum VeFA scaling coefficient  $\|\mathbf{k}\|_\infty$  on image classification tasks.

|                         | UCF101 | Oxford Pets | Oxford Flowers | EuroSAT | DTD   | Caltech101 | Food101 |
|-------------------------|--------|-------------|----------------|---------|-------|------------|---------|
| $\ \mathbf{k}\ _\infty$ | 1.766  | 1.558       | 1.568          | 1.120   | 1.855 | 1.665      | 1.460   |

Table 7: Maximum VeFA scaling coefficient  $\|\mathbf{k}\|_\infty$  on GLUE NLU tasks.

|               | CoLA  | MRPC  | QNLI  | RTE   | SST-2 | STS-B |
|---------------|-------|-------|-------|-------|-------|-------|
| RoBERTa-Base  | 3.889 | 1.879 | 3.256 | 2.693 | 1.522 | 1.527 |
| RoBERTa-Large | 3.028 | 1.671 | 3.061 | 1.886 | 1.544 | 1.404 |

Table 8: Maximum VeFA scaling coefficient  $\|\mathbf{k}\|_\infty$  on NLG tasks.

|                         | GPT-2-Medium | GPT-2-Large |
|-------------------------|--------------|-------------|
| $\ \mathbf{k}\ _\infty$ | 5.233        | 6.171       |